The adsorptive behaviour of electrospun hydrophobic polymers for optimized uptake of estrogenic sex hormones from aqueous media: kinetics, thermodynamics, and reusability study

The adsorptive behaviour of electrospun hydrophobic polymers for optimized uptake of estrogenic sex hormones from aqueous media: Kinetics, thermodynamics and reusability study

Muhammad Yasir*, Fahanwi Asabuwa Ngwabebhoh, Tomáš Šopík, Lenka Lovecká, Dušan Kimmer, Vladimír Sedlařík*

Centre of Polymer Systems, University Institute, Tomas Bata University in Zlín, Třída Tomáše Bati 5678, 76001 Zlín, Czech Republic

*Corresponding authors: M.Yasir (yasir@utb.cz), V. Sedlařík (sedlarik@utb.cz)

Abstract

BACKGROUND: Estrogenic hormones as micropollutants in water systems cause severe adverse effects on human health and marine life, leading to fatal diseases such as breast, ovarian, and prostate cancer. Electrospun polymers have proven high stability and impressive performance in adsorption removal. In this study, electrospun polysulfone (PSU), polyvinylidene fluoride, and polylactic acid were prepared and characterized using SEM, FTIR, TGA, BET, XRD, and porometry.

RESULTS: Nanofibers possess a mean fiber diameter of 149 - 183 nm and a specific surface area of 1.6 - 6.3 m^2/g. The adsorption efficiency of simultaneous removal of estrone (E1), 17β-estradiol (E2), estriol (E3), and 17α-ethinylestradiol (EE2) in a mixed concentration was investigated using HPLC. The results indicate that spun PSU fibers exhibited the highest removal of all four estrogens, with a maximum removal efficiency of 71.2, 65.9, 56.9, and 36.1 % and adsorption capacity of 0.508, 0.703, 0.550, and 0.354 mg/g for E1, EE2, E2, and E3, respectively. Additionally, the adsorption was optimised by varying parameters such as concentration of adsorbate, pH, adsorbent dosage, and temperature to statistically analyse one-way variance using ANOVA. The pseudo-second-order is best fitted for E1, EE2, and E2, while the pseudo-first-order is for E3. The Langmuir-Freundlich isothermal model was most suitable for evaluation, and the thermodynamics depicted the adsorption to be exothermic and spontaneous.

CONCLUSION: The results indicate that spun PSU can be an efficient adsorbent in the simultaneous elimination of estrogens from wastewater and exhibits high regeneration performance of over 60% after six adsorption-desorption cycles.

Keywords: Electrospun nanofibers; kinetics; estrogenic hormones; adsorption mechanism; Wastewater treatment

1. Introduction

Over the past few decades, rapid human population growth and industrialization have resulted in numerous environmental and energy issues. The persistent release of environmental contaminants has severely affected the bio-ecosystem due to their high toxicity and wide occurrence in aquatic environments [1–3]. So far, various toxicants have been classified as posing adverse effects on animals and humans alike [4]. Several investigative reports have detected a high concentration of various types of pollutants such as heavy metals, nitrates, per- and polyfluoroalkyl substances (PFAS), and endocrine-disrupting chemicals (EDCs). Estrogens classified under EDCs are by far the most toxic due to their high bio-toxicity and estrogenicity interfering with the normal functioning of the endocrine systems even at $ng.L^{-1}$ concentrations [5–8]. These estrogenic chemicals exist mainly as estrone (E1), estradiol (E2), estriol (E3), and ethinylestradiol (EE2), and their extensive synthetic use in the treatment of sexual disorders and as contraceptives have resulted in higher than recommended tolerance limit in aquatic resources [9,10]. Globally, these steroids are potentially causing serious health issues by interfering with the naturally released hormones regulating various bodily functions. Several reports suggest that persistent exposure to these anthropogenic chemicals is correlated with serious health issues for humans and animals alike, such as breast cancer, skewed sex ratio, decreased fertility, feminization of males, etc. [11,12].

Considering the above-mentioned highlights, proper remediation of these estrogenic hormones is of immediate scientific concern as less than 1% of the steroids present in the river are expected to be removed by sediments [13]. So far, various strategies have been employed to effectively remove and eliminate steroid hormones, as conventional methods are limited by their high energy cost and low removal efficiency [14,15]. Some of the strategies that have been explored with promising results include UV photolysis, photocatalysis, advanced oxidation process, bio-degradation, nanofiltration, reverse osmosis, and adsorption process [15–17]. Out of these techniques, the adsorption process is considered an environmentally friendly technology with a high removal rate, ease of modification, and low operation cost [18]. Various adsorbent materials have been explored with high adsorption capacity, such as carbonaceous materials, biochar, activated carbon, charcoal, resin, etc. [19–23]. However, these highly adsorbent materials lack sufficient recyclability after a few

cycles and are usually disposed of after a limited life cycle. In this regard, electrospun polymer-based nanofibers have gained popularity for water treatment applications owing to their unique properties such as high surface area, porosity, controlled geometry, and low production cost [24,25]. Out of several methods for nanofibers production, electrospinning is the most common method as nanofibers in controlled dimensions, orientation, and morphology can be obtained [25,26]. For remediation of environmental pollutants, numerous types of polymeric membranes have been synthesized; such as polyvinylchloride, cellulose acetate, polysulfone, polycarbonate, polypropylene, and polydimethylsiloxane [26–31]. Additionally, the polymer-based nanofibers are functionalized with additive materials such zeolite, graphene oxide, ammine groups, etc., to impart unique features to the achieve high removal efficiency and selectivity based on the type of target molecule and application [32–34]. However, little work has been done on investigating the optimized parameters for removing estrogenic hormones using electrospun fibers to eradicate them properly.

In literature, few works have been done with commercial filters of polypropylene, nylon, cellulose acetate, polytetrafluoroethylene, regenerated cellulose, and glass microfibers for the removal of E1 [35]. Another study reported the removal of EE2 by polyamide nanoparticles [36]. Next, polyethersulfone electrospun nanofibers have been used for the adsorption of E2, and polyvinylidene fluoride membrane produced via the phase inversion method and doped with polyvinyl pyrrolidone, and titanium dioxide has been used for the removal of E1 and E2 hormones [37,38]. However, these studies are limited to the removal of a single hormone, and also the works require more in-depth studies related to optimization, kinetics, isotherms, and thermodynamics to understand the mechanisms involved in the adsorption of hormones by electrospun nanofibers and to discuss this matter in more detail. Thus, this gap highlights the necessity of developing electrospun nanofibers for a comprehensive study on the removal of estrogenic hormones.

This study aims to fabricate and test hydrophobic electrospun nanostructures of the thinnest fiber diameter and ample surface area to volume ratio for more adsorption sites. To remove estrogenic hormones from wastewater, we focused on using nanostructured membranes constructed from polymers with strong sorption activity. The goal is to simultaneously adsorb multiple estrogenic hormones from wastewater at neutral pH in a one-step procedure and quantify by HPLC. To understand the characteristics, interactions mechanisms involved, further investigate the feasibility of the results using the experimental data to determine adsorption capacity with contact time and

measure kinetics with appropriate models of pseudo-first-order, pseudo-second-order, intraparticle diffusion, Elovich, and fractional power models. Furthermore, we looked one way variance in ANOVA for optimized adsorption process by varying conditions such as pH, temperature, concentration of adsorbate, and adsorbent dosage to determine a suitable Isothermal model and thermodynamics. Finally, the research evaluates the reusability of prepared spun fibers over six adsorption-desorption cycles to determine their consistent effectiveness and recovery of estrogenic hormones.

2. Materials and Methods

2.1. Materials and reagents

The estrogenic hormones used in this study were purchased from Sigma-Aldrich GmbH, Germany, which includes estrone (E1 ≥99%), 17β-estradiol (E2 ≥98%), estriol (E3 ≥97%), and 17α-ethinylestradiol (EE2 ≥98%). The Kynar Flex® 2801, a copolymer composed of poly (vinylidene fluoride)-co-hexafluoro propylene (PVDF) of molecular weight 455 kDa, was purchased from Arkema (France). Ultrason Polysulfone (PSU) S6010 was purchased from BASF, Germany. Polylactic acid (PLA), Ingeo™ 4060D, biopolymer, was purchased from NatureWorks LLC (USA). N-Methyl-2-pyrrolidone (NMP) was purchased from Sigma-Aldrich, The USA. Acetone and N, N-dimethylformamide (DMF >99.5%) were bought from Lach-Ner, s.r.o., Czech Republic. Sodium tetra-borate decahydrate (borax) and citric acid were purchased from PENTA s.r.o., Czech Republic. The experimental solutions: acetonitrile (HPLC grade), was purchased from Honeywell, Czech Republic, and ethanol (HPLC grade > 99%) from VWR, Czech Republic. Deionized water (pH 7.3, 18.2 MΩ/cm) was sourced from a laboratory Milli-Q ultrapure (Type 1) water purification system, Biopak® Polisher, Merck, The USA. All chemicals were used as received without any further purification throughout the study.

2.2. Preparation of spun nanofibers

First, the conductive components, citric acid and borax (CB) were used to prepare a solution in the ratio of 3:1, respectively. Then, 35 wt% of CB was dissolved in a DMF solution and agitated on a magnetic stirrer for 5 h at 400 rpm. The solution was dropwise used later for adjusting the electrical conductivity of polymeric solutions to optimum prior to electrospinning.

PSU of 20 wt. % was uniformly dissolved in NMP to reach a viscosity of 2 Pa/s and conductivity of 116.3 μS/cm. PLA of 16 wt. % was dissolved in a solution of DMF/Acetone in a ratio of 4:1 to obtain a viscosity of 0.5 Pa/s and an electrical conductivity of 120.1 μS/cm. PVDF 20 wt. % was dissolved in DMF to a viscosity of 1.5 Pa/s and conductivity of 118 μS/cm. Each solution was homogenized in a mixer (Heidolph, RZR 2041) by stirring at 500 rpm for 4h and treated with CB to achieve the reported conductivity values.

Electrospinning was performed on nano spider technology (NS Lab 200S spin line equipment, Elmarco, Czech Republic) equipped with a patented (PCT/CZ2010/000042) rotating electrode comprising spinning elements containing a total of 32 nozzles (16 jets in each row). The process was conducted on a 40 cm wide and 0.14 ± 0.01 mm thick, non-woven antistatic polypropylene (PP) continuous roller collector sheet in the laboratory of Tomas Bata University, Czech Republic, to produce fibers of minimum diameter at optimum operating parameters and the thickness of fibers together with PP substrate sheet was measured to be 0.17 ± 0.01 mm for each material. The applied voltages were 55, 65, and 75 kV for PSU, PLA, and PVDF, respectively. The spacing between electrodes equaled 19 cm, and the rotational speed of collecting PP spun bond was 0.1 m/min to prepare 5 m of each type of electrospun nanofiber in a total duration of 50 min. The pace of solution dosage was set at 0.17, 0.27, and 0.41 mL/min., and the average mass per unit area of the nanofibers reported were 0.59, 1.3, and 1.85 g/m^2, respectively. The operating room temperature was 26 ± 1 °C, with relative air humidity below 30%.

Table 1

Properties of the polymeric solutions.

Sample	Concentration (%)	Density (g/cm^3)	Intrinsic Viscosity (Pa.s)	Electrical conductivity (μS/cm)	Av. mass per unit area (g/m^2)
PSU	20	1.25	2.0	116.3	0.59
PLA	16	1.25	0.5	120.1	1.30
PVDF	20	1.78	1.5	118.0	1.85

2.3. Characterization methods

2.3.1. Fourier-transform infrared spectroscopy (FTIR)

FTIR analysis was conducted using a Ge crystal in attenuated total reflectance (ATR) mode on a Nicolet 320 spectrometer (ThermoScientific, USA). Adsorption of the estrogenic hormones on the surface of polymeric nanofibers was tested to determine the functional groups involved in the interaction. Spectra were recorded across 400 - 4000 cm^{-1} under standard conditions with resolution and scan rate set at 4 cm^{-1} and 16, respectively.

2.3.2. Scanning electron microscopy (SEM)

Nova 450 scanning electron microscope (SEM) (FEI, Thermo Fisher Scientific, USA) was used to image electrospun fibers to observe the surface morphology and the defects such as beads in the structures that might incorporate during electrospinning and to determine the desired diameter of fibers. The electron beam was operated at an accelerating voltage of 5 - 10 kV with a through-the-lens detector (TLD). The mean diameter of fibers was measured via ImageJ version 1.52a software.

2.3.3. BET Surface Area and Porosity Analysis

Surface area and fiber surface pore diameter analysis were performed according to the Brunauer-Emmett-Teller (BET) method. To determine these quantities, a highly precise analyzer (BELSORP-mini II, BEL Japan Inc., Japan) was used for specific surface area and pore size. Outgassing of the substrate was carried out for 12 h in a vacuum at 100°C before starting measurement. Furthermore, according to ASTM F316-03 (2011), the pore size distribution of nanostructures and air permeability was tested and assessed by flow porometer NV, Belgium using Galpor as a wetting liquid.

2.3.4. X-Ray Diffraction

X-ray diffractogram (XRD) of electrospun fibers were recorded over the angle 2θ ranging from 5 - 90° via CoK_{β} (λ=1.79 Å) as a source in Miniflex^{TM} 600 X-ray diffractometer (Rigaku, Japan). The operating parameters such as voltage, current, step time, and step size were 40 kV, 15 mA, 10°/s, and 0.02°, respectively.

2.3.5. Thermogravimetric analysis

To obtain the thermal stabilities of produced nanofibers, a TGA Q500 thermogravimetric analyzer (TA Instruments, USA) was used with samples mass ranging from 12 - 20 ± 0.5 mg, depending on their densities. The samples were heated from 25 to 700 °C in an alumina crucible at a ramp of 15 °C/min under N_2 flow of 100 mL/min.

2.3.6. High-Performance Liquid Chromatography (HPLC) analysis

HPLC analysis of hormones (E1, E2, EE2, and E3) calibration standards and samples were carried out on an HPLC DionexUltiMate 3000 Series (Thermo Fisher Scientific, Germany). The separation was performed on a reversed-phase column Kinetex 2.6u C18 100 A (150x4.6mm; Phenomenex USA) equipped with a security guard column (Phenomenex. USA) at 30 °C. A combination of HPLC grade water and acetonitrile was used as the mobile phase (55:45, v/v) at a flow rate of 0.8 mL/min with an isocratic run time of 12 min. The sampler chamber was fixed at 5 °C, and a 20 µL of volume was injected onto the column. Samples were performed in triplicates and elutes were analyzed using a wavelength of 200 nm to quantify the hormones' mean concentration by plotted calibration curve in Chromeleon software version 7.2 (Thermo Fisher Scientific, USA) [39].

For a preliminary test, a mixture of hormone solution was prepared to contain 0.2 mg/L of each hormone with a total concentration of 0.8 mg/L and left for magnetic stirring overnight at 700 rpm, followed by 30 min of sonication before storing it in a dark place. Samples were collected via a micropipette (HTL Lab Solution, Poland) and passed through a glass microfiber (GMF) filter (Whatman, Czech Republic) with 25 mm of diameter and 0.45 µm of pore size before dosing into 1.5 mL screw neck vials (VWR, Czech Republic). Later for optimization studies, a single high concentrated E1 (0.5 mg/L) solution was prepared as a stock solution that was diluted to prepare several different concentrations to test variation in adsorbate concentration (E1).

2.4. Adsorption study of spun polymeric nanofibers

Batch adsorption tests were conducted to determine the adsorption efficiency and capacity of each estrogenic hormone on spun nanofibers. Studies were performed similarly as detailed in previous work [39]. 20 mg of each electrospun nanofibers were supplemented into 250 mL conical flasks filled with 100 mL solution from the prepared stock. The flasks were continuously agitated at 200 rpm

on an orbital incubator shaker (Stuart® S1500, Barloworld Scientific Ltd., UK). The influence of varying different parameters such as initial concentration of hormone (mg/L), solution pH, adsorbent dosage (mg), and temperature of adsorbate solution (°C) was observed on the adsorption removal. Samples were withdrawn at predetermined time intervals using an optimized protocol to collect in vials via a GMF syringe filter and measure the remaining concentration of estrogenic hormones present in the experimental flask. 4 mL of withdrawn sample was substituted with 4 mL of ultrapure water at each interval. To ensure precise results, the first 2 mL of the filtrate was passed through the GMF filter and discarded to avoid self-adsorption or residual permeate left during the previous sampling. A set of triplicates of "control" solution flasks were also included in the experimental run to obtain the initial reference mean concentration. The mean concentration values with standard deviation using Gaussian distribution were recorded and reported with reference to control. The calculated percentage adsorption removal and equilibrium adsorption capacity of each hormone at a given time (t) was determined by the expression in Eq. (1) and (2), as follows:

$$Removal\ (\%) = \frac{C_i - C_t}{C_i} \times 100 \tag{1}$$

$$q_e = v \times \frac{C_i - C_e}{m} \tag{2}$$

where C_i is the initial concentration (mg/L), and C_t is the concentration at time t (mg/L). The mass of adsorbent (m) in grams and v is the volume of solution in liters and q_e is equal to the equilibrium adsorption capacity in the adsorption process.

2.5. Adsorption kinetics study

The experimental results data were evaluated to study the factors involved in the adsorption process, such as mass transfer and types of chemical interactions, to determine the rate-limiting step. Thus, kinetics models help select optimized parameters and conditions required for full-scale elimination of the estrogenic hormone process. However, choosing the parameters and concluding the mechanisms involved in the complex heterogeneous systems is much more complicated because of superimposed surface effects on the chemical effects. Therefore, to this concern, five models were deployed; Pseudo-first-order, Pseudo-second-order, Weber-Morris intra-particle/membrane diffusion, Elovich, and Fractional power model equations were best fitted with

the experimental data to evaluate the simultaneous uptake of four estrogenic hormones by PSU fibers. The mentioned models are popular in describing the nature of aqueous/solid systems. Thus, these models can be expressed by the Eq. (3), (4), (5), (6), and (7), respectively.

The pseudo-first-order introduced by Lagergren is the most common and widely used model for such hormones' adsorption study. It explains that the rate of estrogenic hormone adsorption on the surface of PSU fibers is directly dependent on the number of hormones adsorbed from the solution phase [40].

$$q_t = q_e(1 - e^{-k_1 t}) \tag{3}$$

Where q_t is the amount of hormone adsorbed per unit mass at time t (mg/g), q_e is the amount of hormone adsorbed per unit mass at equilibrium (mg/g), k_1 is the first-order rate constant (L/min).

In contrast, the pseudo-second-order equation explains the hormone adsorption capacity and can exclusively predict the kinetic behavior over a long period. This model implies that surface adsorption is the rate-determining step owing to chemisorption as a consequence of physicochemical interactions between the PSU fibers and the hormone solution phase [41].

$$\frac{t}{q_t} = \frac{1}{k_2 {q_e}^2} + \frac{t}{qe} \tag{4}$$

Where k_2 is the second-order rate constant (g/(mg min)).

Next, the Weber-Morris intra-particle/membrane diffusion is a diffusion-controlled model; it suggests that the rate of adsorption is proportional to the speed of adsorbate with which it can diffuse towards the surface of the adsorbent. Primarily, the adsorption process occurs in a sequence of steps; first, the adsorbate moves from the bulk of the solution to the surface of the adsorbent and then diffuses through the boundary layer to the outer surface of the adsorbent. Meanwhile, the adsorbate adsorbs on the active sites of the adsorbent and diffuses to penetrate through the pores. It is essential for the validity that the linear convergence line of the best fit plotted for estrogenic hormone must intersect the coordinates of origin; then, this model is considered to be the rate-determining step [42].

$$q_t = k_3 t^{0.5} + C \tag{5}$$

Where k_3 is the intra-particle reaction rate constant (mg/g $h^{1/2}$), C is the y-intercept constant (mg/g) which gives the information about the boundary layer thickness.

Furthermore, in interactions where chemisorption is the only dominant mechanism for the adsorbate to be deposited on the surface of the adsorbent without desorption of products, then the rate of adsorption gradually decreases with time due to the surface layer coverage. In such cases, the Elovich model is the most suitable for explaining the chemisorption process [43].

$$q_t = \beta \ln(\alpha\beta) + \beta lnt \quad (6)$$

In Eq. 6, α and β are the coefficients such that α represents the initial adsorption rate (g/mg min)) and β represents the desorption coefficient (mg/(g min)). These coefficients can be calculated from the slope and y-intercept of the plots, respectively.

Lastly, the fractional power model is the modified and advanced form of the Freundlich equation [44].

$$lnq_t = lna + blnt \quad (7)$$

In Eq. 7, a and b are the coefficients in the expression at the given condition that $b < 1$, the product of a and b is defined as the specific adsorption rate at a time of 1 min after the experiment is initiated.

2.6. Thermodynamic study

The impact that surrounds temperature influences the adsorption capacity of spun PSU was studied in a temperature-controlled system at 25, 35, and 45 °C. The thermodynamics of the adsorption process were estimated using the following equations [45,46].

$$K_D = \frac{C_s}{C_e} \quad (8)$$

$$lnK_D = -\frac{\Delta H}{RT} + \frac{\Delta S}{R} \quad (9)$$

$$\Delta G = \Delta H - T\Delta S \quad (10)$$

Where, ΔG is the Gibbs free energy change, ΔH is the enthalpy change, and ΔS entropy change. K_D is the distribution coefficient (a ratio of solid phase to solute concentrations), R (8.314 J/mol K) is the universal gas constant, C_s (mg/L) is the concentration of the hormone on the adsorbent, and T (K) is the absolute temperature.

2.7. Isotherm modeling

The adsorption isotherm study was performed at the initial pH of 7, the temperature of 25 °C, and different initial concentrations of the E1 hormone mixture (0.1, 0.2, 0.3, 0.4, and 0.5 mg/L). Spun PSU was used as the adsorbent, and samples were collected after 9 h of adsorption. The fitting of the adsorption equilibrium data was evaluated using the Langmuir and Freundlich isotherms. The non-linear regression equations used for the models are shown in Eq. (11) and (12), respectively [47–49]:

$$q_e = \frac{Q_{max} K_L C_e}{(1 + K_L C_e)} \tag{11}$$

$$q_e = K_F C_e^{1/n} \tag{12}$$

Where, q_e is the amount of adsorbed hormone on PSU adsorbent at equilibrium (mg/g), C_e is the residual equilibrium hormone concentration (mg/L), Q_{max} is the maximum adsorption capacity (mg/g), K_L is the Langmuir isotherm constant, K_F is the Freundlich constant and n is the Freundlich heterogeneity factor.

2.8. Reusability study

For the desorption test, the nanofibers were extracted from the conical flasks containing the hormone solutions and washed thoroughly with distilled water, followed by gentle stirring at a constant 100 rpm for 10 min in a 100 mL mixture of 1:1 water and ethanol to remove the hormones entirely and eluted in the mixture. Finally, the nanofibers were placed in 100 mL of water until the next adsorption cycle. The procedure was repeated for six consecutive adsorption-desorption cycles. The consecutive adsorption cycles were performed at optimum conditions of pH 7, temperature 35, 0.2 mg/L concentration of adsorbate (E1), and 40 mg dosage of adsorbent (PSU).

2.9. Statistical analysis

The data are displayed as Mean ± Standard error. OriginLab software version 9.0 was used for statistical analysis. The difference between values was determined by a one-way analysis of variance (ANOVA). A value of $p < 0.05$ was determined as statistically significant [50].

3. Results and discussion

3.1. Characterization of materials

3.1.1. SEM analysis

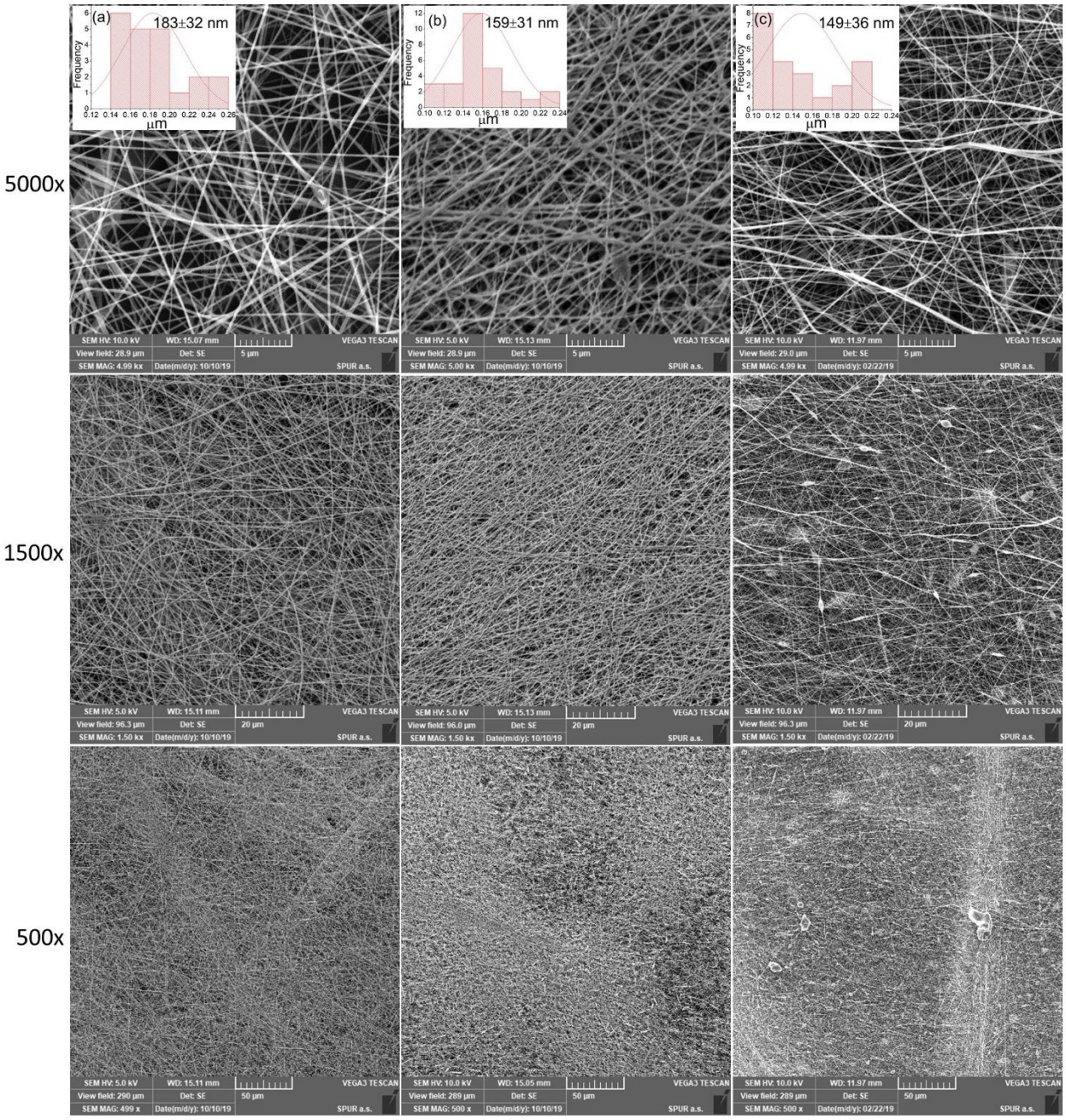

Figure 1. Electron micrographs with (inset) distribution of frequency size of the electrospun nanofibers (a) PSU, (b) PLA, and (c) PVDF at different magnifications of 500x, 1500x, and 5000x.

Figure 1 reveals that the electrospun nanofibers were produced without beads or defects, as desired. The calculated average fiber diameters from SEM were in the range of 149-183 nm, which are firmly in compliance with the range of electrospun nanofiber (174-330 nm) reported in the literature [39]. These low achieved diameters are attributed to the optimized parameters used to prepare electrospinning solutions, including low polymer concentration in the solution, intrinsic viscosity, and electrical conductivity. Further properties are mentioned in Table 2.

Table 2

SEM, BET, and porometry data of electrospun polymeric fiber materials.

Nanofiber	**Average fiber diameter SEM (nm)**	**Porometry Mean pore size (μm)**	**Air permeability (l/cm^2.min.bar)**	**BET surface area (m^2/g)**
PSU	183 ± 32	0.91	244	6.267
PLA	159 ± 31	1.10	197	0.302
PVDF	149 ± 36	0.39	077	1.612

It can be seen in Table 2 that the mean pore size ranged from 0.39 - 1.10 μm and air permeability from 77-244 l/cm^2.min.bar, which are inversely dependent on the average mass of nanofiber per unit area (Table 1), the relative structural porosity is also visible in SEM micrographs at the same magnification. The measured BET surface area ranged from 0.3 - 6.3 m^2/g, which is directly dependent on the intrinsic viscosities of the solutions (PSU ~2.0, PLA ~0.5, and PVDF ~1.5 Pa.s) prior to electrospinning. The effect of the surface area is also evident in the preliminary test for the adsorption of hormones, where PSU was observed to adsorb and remove the highest percentage of hormones.

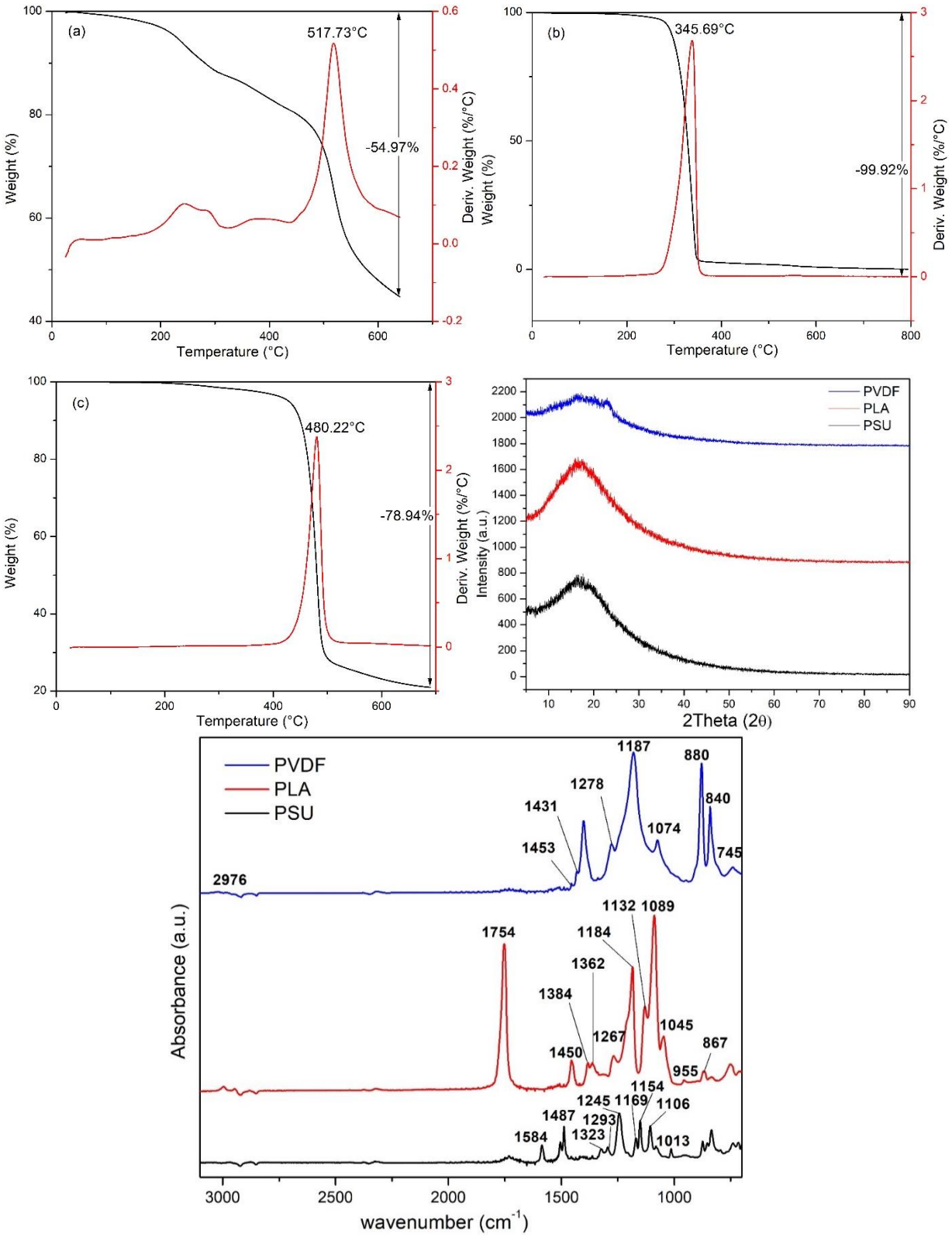

Figure 2. Thermogravimetric analysis of (a) PSU, (b) PLA, and (c) PVDF, (d) X-ray diffractograms, and (e) FTIR spectra of the different electrospun nanofibers.

To investigate the physiochemical features of electrospun nanofibers. The TGA graphs in Figures 2 (a, b, and c) displayed that no nanofibers degradation was observed up to 100 °C for any polymer. A slight initial dip in Figures 2a, b, and c is due to the evaporation of water, while the weight loss started at around 200 °C for PSU, about 300 ℃ for PLA, and nearly 400 ℃ for PVDF, which is far above the tested experimental range for adsorption in this study. Additionally, the degradation with a rapid weight loss was observed at 517.73, 345.69, and 480.22 °C for PSU, PLA, and PVDF, respectively. The XRD (Figure 2d) also revealed that a broad peak region was observed for each polymer around 2θ = 17-20°, which indicates the semi-amorphous nature of the polymer electrospun nanofibers. For PVDF, two broad spikes are seen at around 18° and 22° that belong to the α and β phases, respectively [51].

The IR spectra in Figure 2e shows characteristic peak at about 2974 cm^{-1} assigns to CH_2 symmetric stretching present in all three polymeric nanofibers. Then, the spike at 1453 cm^{-1} for PVDF is the scissoring or in-plane bending of CH_2 in the α-phase. Furthermore, the rocking of CH_2 or CF_2 asymmetric stretching is observed at 840 cm^{-1}, and in-plane bending at 745 cm^{-1} is seen in the β-phase [52]. PVDF appears in different crystal phases; the spike at 840 cm^{-1} is considerably large, representing the β-phase, as well as the peaks at 1431 and 1278 cm^{-1} define the crystalline phase. The peak at 1074 cm^{-1} is mainly due to the β-phase, but traces of other phases could also be found around this location in the literature [51]. The absorption peak at 1187 cm^{-1} is due to the combination of β and γ phases, and the large peak at 880 cm^{-1} is a result of the combination of all existing phases. Whereas, peaks at 840 and 1278 cm^{-1} are the usual β-phase peaks [53].

In PLA, the characteristic peaks observed at 1754, 1267, and 754 cm^{-1} assigned to –C=O are due to the strength vibration, bending vibration, and torsion vibration, respectively. The peak located at 955 cm^{-1} corresponds to C–C group. In addition, the spikes at 1132, 1045, and 867 cm^{-1} belong to C–O groups for strength vibration. The deformation of C-H appears at 1450 cm^{-1}, and the symmetric and asymmetric strength vibration of the –CH bond are indicated at 1362 and 1384 cm^{-1}. The formed peaks at 867 and 754 cm^{-1} are evidence of the amorphous and crystalline regions present in PLA, respectively [54].

The spectra peak intensity for PSU revealed at 1323 and 1293 cm^{-1} corresponds to the asymmetric absorption of the S═O group, while the peak at 1169 cm^{-1} belongs to the symmetric absorption of

the S═O group. In addition, the characteristic absorption peaks at 1584 and 1487 cm^{-1} are attributed to the benzene rings [55]. The main characterized peaks are present at 1584, 1245, 1323, 1154, 1106, and 1013 cm^{-1}, corresponding to the stretching caused by aromatic C=C, C-O-C (ether group), and O=S=O bonds, respectively [56].

3.2. Batch adsorption studies

3.2.1. Preliminary adsorption for different prepared polymeric nanofibers

To evaluate and distinguish the efficiency of the prepared spun PSU, PLA, and PVDF nanofibers, short-term batch tests using the materials were performed to ascertain their adsorption efficiency against four different hormones of E1, E2, EE2, and E3. According to deduced results (Figure 3a), spun PSU showed more than 50% removal efficiency for almost all studied hormones. Removal efficiency for the different spun nanofibers was in the magnitude of PSU>PLA>PVDF. Based on this initial evaluation, spun PSU material was used for subsequent study due to its high adsorption capacity for different estrogenic hormones.

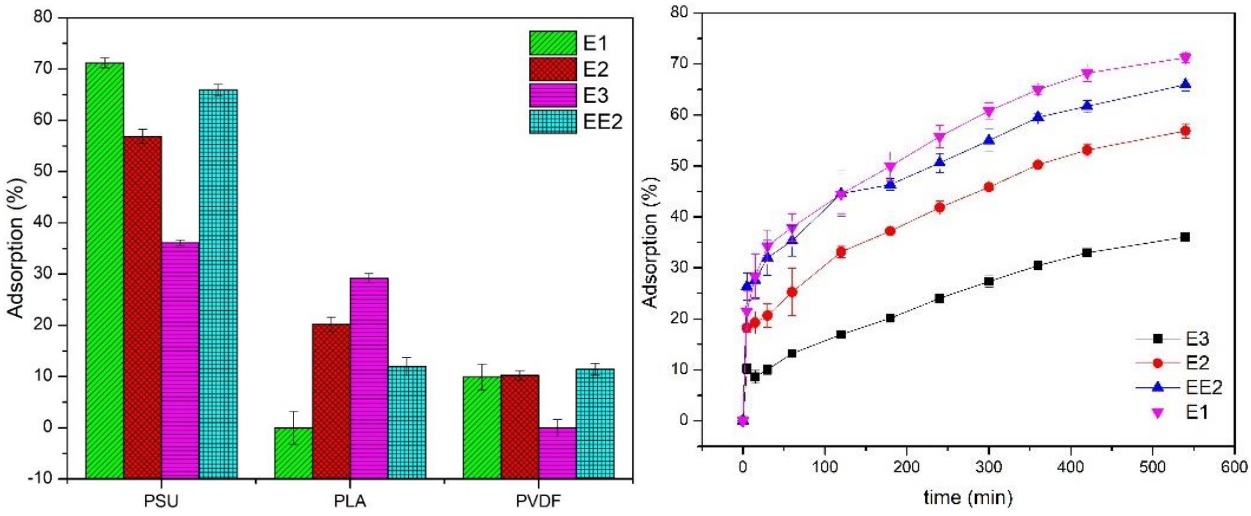

Figure 3. (a) Comparative adsorption efficiency of hormones (E1, E2, E3, and EE2) on PSU, PLA, and PVDF electrospun nanofibers (left panel), and (b) Adsorption efficiency trends of E1, E2, E3, and EE2 hormones on PSU nanofibers as a function of time (right panel). (pH: 7, concentration of each hormone: 0.2 mg/L, and testing duration: 9 h)

3.2.2. Effect of contact time

The contact time plays a major role in the adsorption of the hormones onto the different spun nanofibers. The effect of contact time on the adsorption of the various hormones (E1, E2, EE2,

and E3) by spun PSU as the adsorbent with the highest adsorption capacity was further investigated and is shown in Figure 3b. It can be observed that the initial uptake of the hormones occurred within the first 2 h, and after that, a gradual increase with time up to 9 h depicted as apparent equilibrium. This initial rapid uptake of the hormones could be due to the availability of the adsorption sites on the adsorbent materials. It was evident that the adsorbed amount of the hormones adsorbed onto the adsorbent increased by increasing the contact time. After 4 h, the removal of the hormones from the aqueous phase was more than 50%. The removal capacity of PSU for the different hormones was in the magnitude of E1>EE2>E2>E3. This indicated that the E1 hormone had the highest binding affinity to PSU. This may be due to the stoichiometric structural arrangement of the E1 hormone molecule that favored more hydrogen bonds and π-π interaction with the adsorbent [39].

3.3. Adsorption kinetics

The adsorption of estrogenic hormones on PSU increased with time until equilibrium was achieved. The initial rate was fast for 60 min, and then it gradually decreased with an increased contact time, assuming saturation at 540 min. The adsorption kinetic plots for the adsorption of E1 on PSU nanofibers are shown in Figure 4, and the obtained kinetic parameters from the models mentioned above are presented in Table 3.

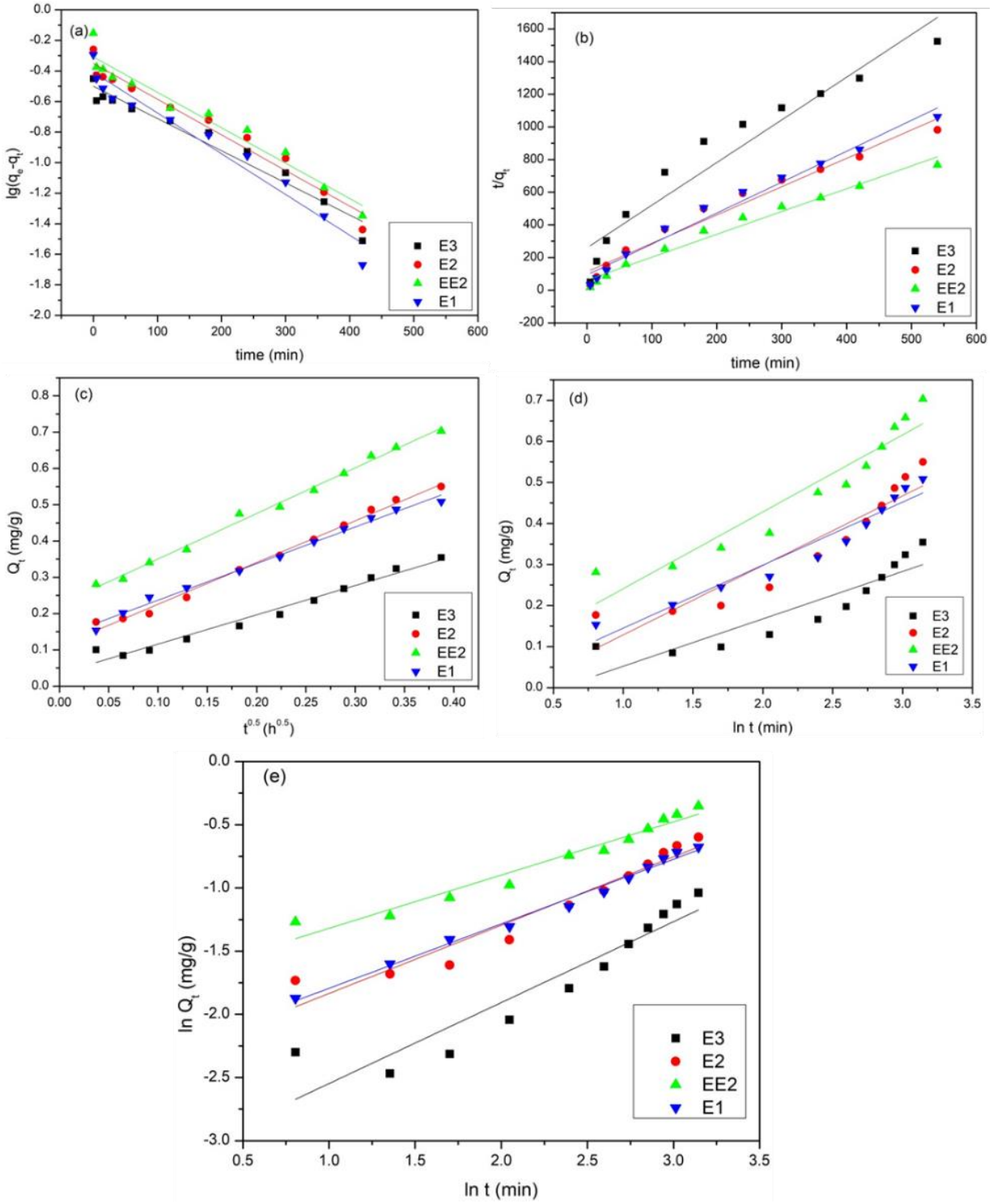

Figure 4. Adsorption kinetics plots of the four estrogenic hormones (E1, E2, EE2, E3) on PSU nanofibers, (a) Pseudo-first-order, (b) Pseudo-second-order, (c) Weber-Morris intraparticle diffusion, (d) Elovich, and (e) Fractional power model.

Several kinetic models were used to investigate the experimental data that can best fit to understand the ability of concomitant adsorption of estrogenic hormones on the surface of PSU fibers. In Figure 4a, the plotting *In* $(q_e\text{-}q_t)$ vs. t shows a strong agreement of E3 hormone with a linear best fit line covering the data set points, and the predicted adsorption capacity of 0.307 mg/g is close to the experimental equilibrium adsorption capacity of 0.354 mg/g with a high regression coefficient of 0.954. Whereas, the theoretical adsorption capacities for E1, E2, and EE2 are 0.367, 0.423, and 0.451, which are unsatisfactory and reasonably less expected compared to the experimental values of 0.508, 0.550, and 0.703 mg/g, respectively. However, the rate constant K_1 is precise and similar for each estrogenic hormone, but the data set points do not match the generated lines of best fits for E1, E2, and EE2 for the pseudo-first-order equation.

For Figure 4b, the plots of t/q_t vs. t must be linear lines to accurately and precisely estimate the q_e and k_2 values from the slopes and y-intercepts of each data set, respectively. The results obtained clearly indicate that E1, E2, and EE2 estrogenic hormones follow Pseudo-second order model kinetics. The data set points mostly match the lines of best fit with a high regression coefficient of 0.962, 0.970, and 0.975 for E1, E2, and EE2, respectively. Also, the calculated adsorption capacities of 0.528, 0.576, and 0.715 are strongly in compliance with the experimentally achieved values of 0.508, 0.550, and 0.703, respectively. The slightly lower values obtained during the experiment are referred to as the inhomogeneous active sites on the surface of PSU because the rate of adsorption is primarily dependent on the concentration of hormone solution and the number of available active sites present on the surface of the adsorbent material. Similar results have been observed and reported by Al-Khateeb *et al.* in the literature using MWCNTs as an adsorbent for these hormones. The adsorption capacities reported were 0.423, 0.472, and 0.472 for E1, E2, and EE2, respectively [43]. Furthermore, E3 shows a clear mismatch using the pseudo-second-order model. The data points do not fit the linear best fit line, and in fact, two separate portions are observed; one for the first 120 min and the second from 180 min till the end of the experiment. The plots in Figure 4b were used to determine the rate constants (k_2) and the calculated equilibrium adsorption capacities (q_e) expressed in Eq. (4) to obtain the regression coefficient (R^2) shown in Table 3.

The plot of q_t vs. $t^{0.5}$ is shown in Figure 4c, representing the intraparticle diffusion model. The linear plots of all estrogenic hormones have a high regression coefficient of 0.992, 0.993, 0.995,

and 0.975 for E1, E2, EE2, and E3, respectively, but the plots do not intercept through the origin. This indicates that intraparticle diffusion is involved in the adsorption process, but it is only a part of the mechanism and is not wholly the rate-determining step. The plausible reason could be that estrogenic hormones do not converge properly. This could be due to the surface boundary layer effects that might have dominated the interaction of the adsorption process in the latter half. Therefore, the diffusion rate decreases as the adsorption progresses, and a gentle slope is observed because of the low concentration of estrogenic hormones remaining in the solution.

The plot in Figure 4d of q_t vs. *lnt* depicts high adsorption rates per minute, which indicates and elucidates that chemisorption is the most dominant adsorption mechanism in the interaction of estrogenic hormones with PSU nanofibers. EE2 had the highest adsorption capacity of 0.703 mg/g and an initial adsorption rate of 18.870 g/mg.min. The descending order of removal rates is in the magnitude of EE2>E1>E2>E3, with E1 having the highest regression coefficient of 0.942 and the highest overall adsorption removal percentage (Figure 3) owing to its binding affinity to PSU. The plausible reason could be the stoichiometric structural arrangement of the E1 molecule that favored more hydrogen bonds and π-π interactions with the PSU fibers based on its structure.

In Figure 4e, the plots of lnq_t vs. *lnt* are represented. As can be seen, an entire mismatch is evident for most of the estrogenic hormones, except for E1, where a linear relationship is seen with a regression coefficient of 0.990, but the adsorption capacity is unsatisfactory. This indicates that the fractional power model is not appropriate for these estrogenic hormones. The calculated parameters using Equations (3), (4), (5), (6), and (7) are shown in Table 3.

Table 3

The kinetic models' parameters with each hormone using PSU electrospun nanofibers.

Models parameters	**Hormones**			
	E1	**E2**	**EE2**	**E3**
q_e, expt (mg/g)	0.508	0.550	0.703	0.354
Pseudo-First Order model				
k_1 (min^{-1})	0.003	0.002	0.002	0.002
q_e, cal (mg/g)	0.367	0.423	0.451	0.307
R^2	0.962	0.970	0.975	0.954
Pseudo-Second Order model				
k_2 (g/mg.min)	0.038	0.027	0.031	0.026
q_e, cal (mg/g)	0.528	0.576	0.715	0.383
R^2	0.980	0.968	0.981	0.929

Intraparticle diffusion model				
k (mg/g $h^{0.5}$)	1.009	1.152	1.256	0.807
I (mg/g)	0.136	0.110	0.225	0.035
R^2	0.992	0.993	0.995	0.975
Elovich Model				
α (g/mg.min)	11.641	7.302	18.870	5.796
β (mg/g.min)	0.077	0.085	0.094	0.058
R^2	0.942	0.881	0.909	0.819
Fractional power model				
a	0.100	0.093	0.176	0.041
b	0.255	0.270	0.210	0.320
a+b	0.025	0.025	0.037	0.013
R^2	0.990	0.939	0.957	0.885

3.4. Adsorption based on the variation of single parameters

Following the preliminary adsorption, contact time, and kinetic studies, the E1 hormone was selected as the most suitable hormone for further investigation of adsorption due to high interaction with the adsorbents, leading to the highest removal efficiency. As one of three major endogenous estrogens found in humans, this hormone serves as a suitable candidate. Different adsorption parameters of solution pH, hormone concentration, adsorbent dosage, and temperature effect were investigated by varying one factor and keeping the others constant.

3.4.1. Effect of solution pH

Solution pH is a vital index controlling parameter for the adsorption performance of an adsorbent. The solution pH was varied from 3 to 9 at a constant dosage of 20 mg, 0.2 mg/L hormone concentration, pH 7, and temperature 25 °C under shaking at 150 rpm. Figure 5a reveals that the hormone uptake by PSU is slightly affected by the initial solution pH ranging from 3.0 to 7.0, while the adsorption efficiency significantly increased from pH 7 to 9. The lowest removal efficiency was observed at pH 3 at 44.32% compared to 79.92% determined at pH 9.0. This observation can be traceable to the ionization state of the estrone (E1) hormone molecule. Generally, estrogen hormones are considered weak Lewis acid, and their ionization state is strongly dependent on solution pH. The reported value in literature for pKa of E1 is approximately 10.34 [57]. pKa represents the acid dissociation constant of E1, which above this value, the hormone deprotonates and becomes negatively charged, thereby losing its hydrogen atom affinity. As such, the adsorption study was investigated below pH 9 to favor interaction between the hormone

molecules and the adsorbent materials [58]. Though maximum adsorption was achieved at pH 9, for environmental and better safety handling of the system, pH 7, which shows more than 50% removal efficiency, was selected as the most suitable solution pH.

3.4.2. Effect of hormone concentration

The effect of the initial concentration of the hormone on spun PSU adsorption properties was investigated as presented in Figure 5b. According to the plot, the amount of hormone adsorbed on spun PSU was evaluated by varying initial concentrations from 0.1 to 0.5 mg/L at a dosage of 20 mg, pH 7, and temperature of 25 °C under shaking at 150 rpm. It was observed that the amount of hormone adsorption increased with an increase in initial concentration. However, the removal efficiency decreases with an increase in initial hormone concentration. As seen depicted in Figure 5b, the removal efficiency decreased from 52.95% to 48.62%. This phenomenon was attributed to the gradual saturation of the adsorbent adsorption sites with an increase in initial hormone concentration [59].

3.4.3. Effect of adsorbent dosage

Dosage of adsorbent plays a crucial role in the whole adsorption process. Investigations were performed by varying the amount of spun PSU (10, 20, 30, and 40 mg) while keeping the other factors constant at 0.2 mg/L, pH 7, and temperature 25 °C under shaking at 150 rpm. Figure 5c shows that increasing the amount of adsorbent led to increased adsorption capacity. This is ascribed to more available adsorption sites as the amount of the adsorbent increases, allowing for an increase in the number of hormone pollutants attached to the adsorbent [60]. It is evident that increasing the amount of the adsorbent directly increases the adsorption surface giving rise to an increased removal percentage of the hormone from an aqueous phase. The removal efficiency rises from 37.42% to 79.82% by increasing the adsorbent amount from 10 mg to 40 mg. In addition, it was observed that the removal percentage was greater than 50% using adsorbent amounts ≥ 20 mg.

3.4.4. Effect of temperature

The effect on removal efficiency of the hormone by spun PSU was investigated by varying the medium's temperature (25, 35, and 45 °C) at constant 20 mg, 0.2 mg/L, and pH 7 under shaking at 150 rpm. Based on obtained results (Figure 5d), low temperatures (25 and 35 °C) favoured

higher adsorption capacity as compared to a decrease in adsorption at elevated temperatures (45 °). This observation was mainly attributed to the exothermic nature of the adsorption process [61]. In addition, low adsorption at elevated temperatures may relate to the denaturing of the molecular hormone structure, affecting binding affinity to the adsorbent adsorption sites. The adsorption efficiency of the hormone was most significant at 35 °C, with a removal capacity of 65.33% compared to 40.26% for higher temperatures. This suggested that adsorption at mild room temperature best suited the removal of the hormone, and continued heating would decrease the adsorption efficiency. Thus, for economic and environmental considerations, the best conditions for removing the estrogenic hormone were suitable for temperatures between 25 – 35 °C.

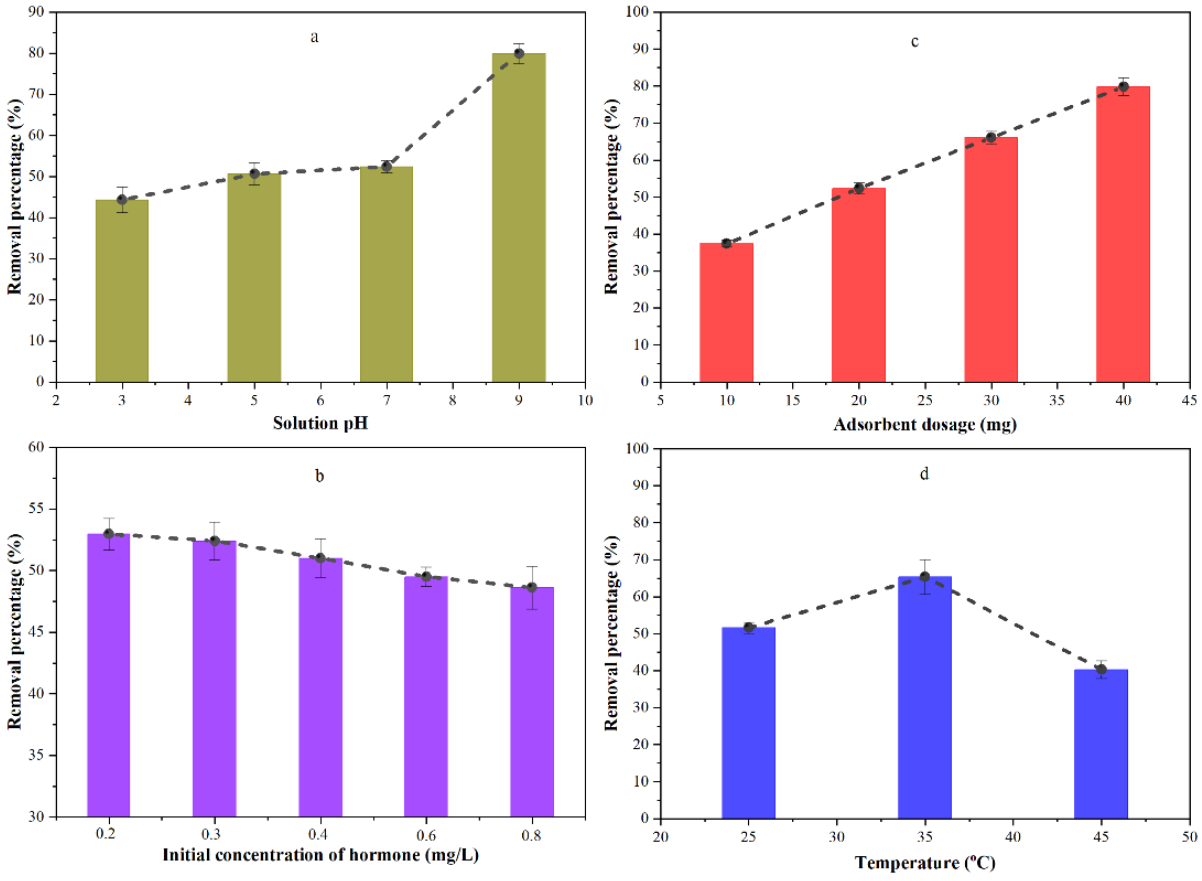

Figure 5. Effects of different adsorption parameters: a) solution pH, b) initial adsorbate concentration, c) adsorbent dosage, and d) temperature on the removal of E1 hormone using spun PSU nanofibers.

3.5. Adsorption mechanism

The types of mechanism depend on several factors such as the hydrophobic nature of the hormone, surface area of the polymeric nanofiber available for active sites interaction, functional groups present on hormone and nanofiber, and pH of the solution. There can be more adsorption mechanisms present together that contribute and can lead to the adsorption of E1 on PSU nanofibers as shown in Figure 6. Size exclusion can contribute to a negligible amount of adsorption on the surface of PSU nanofibers (BET mean pore diameter on fiber surface was 10.288 nm and SEM mean fiber diameter equaled 183 ± 32 nm). This is expected because the reported diameter size of the E1 molecule in literature is approximately 0.8 nm using the Stokes-Einstein equation [62]. Thus, a minuscule amount of E1 molecules can be entrapped in the pores on the fibers' surface. However, most of the E1 molecules can readily pass through the porous non-woven structure of nanofibers owing to its mean porosity of 0.91 μm and similarly for PLA (1.10 μm) and PVDF (0.39 μm). Additionally, the dissociation of hydroxyl groups of E1 attached to its aromatic rings is dependent on the acid dissociation constant (pK_a); this value of E1 is 10.34, which is higher than that of phenol (pK_a = 10). This indicates that E1 would not deprotonate and stay predominantly neutral at pH <10.5; therefore, the influence of electrostatic charge is absent in this system. The other possibility of E1 adsorption on the PSU internal and external surfaces could be due to the hydrophobic interactions; the log K_{ow} (octanol-water partitioning coefficient) is 3.43, which is a greater value than 2.5; therefore, it suggests that E1 could readily be adsorbed on hydrophobic surfaces of PSU, PLA and PVDF nanofibers. Next, the electron-rich and deficient benzene aromatic rings possessed by both adsorbate (E1) and the adsorbent (PSU) will lead to π–π interactions by overlapping double-bonded C=C atoms present in the two molecules. Furthermore, the phenolic hydroxyl and carbonyl functional groups present on E1 can facilitate the formation of hydrogen bonding by acting as either a proton donor or acceptor. However, in this case, the -OH terminal group present in E1 molecules will serve as a proton donor and bind with the groups containing highly electronegative oxygen atoms in the structure of PSU nanofibers [62]. Similarly, the C=O bond present at 1754 cm^{-1} in PLA (Figure 2e) is responsible for its hydrogen bonding with hormones; however, this interaction is absent in the case of PVDF. This is the strongest of all the interactions and provides a boost in the rapid adsorption of the E1 hormone. Similar hydrogen bonding interactions of nylon 6,6 membrane and electrospun polyurethane fibers with

E1 are reported in the literature [35,39]. Hence, a similar interaction behavior is expected to occur in the remaining hormones (E2, EE2, E3) of the same estrogenic family [57].

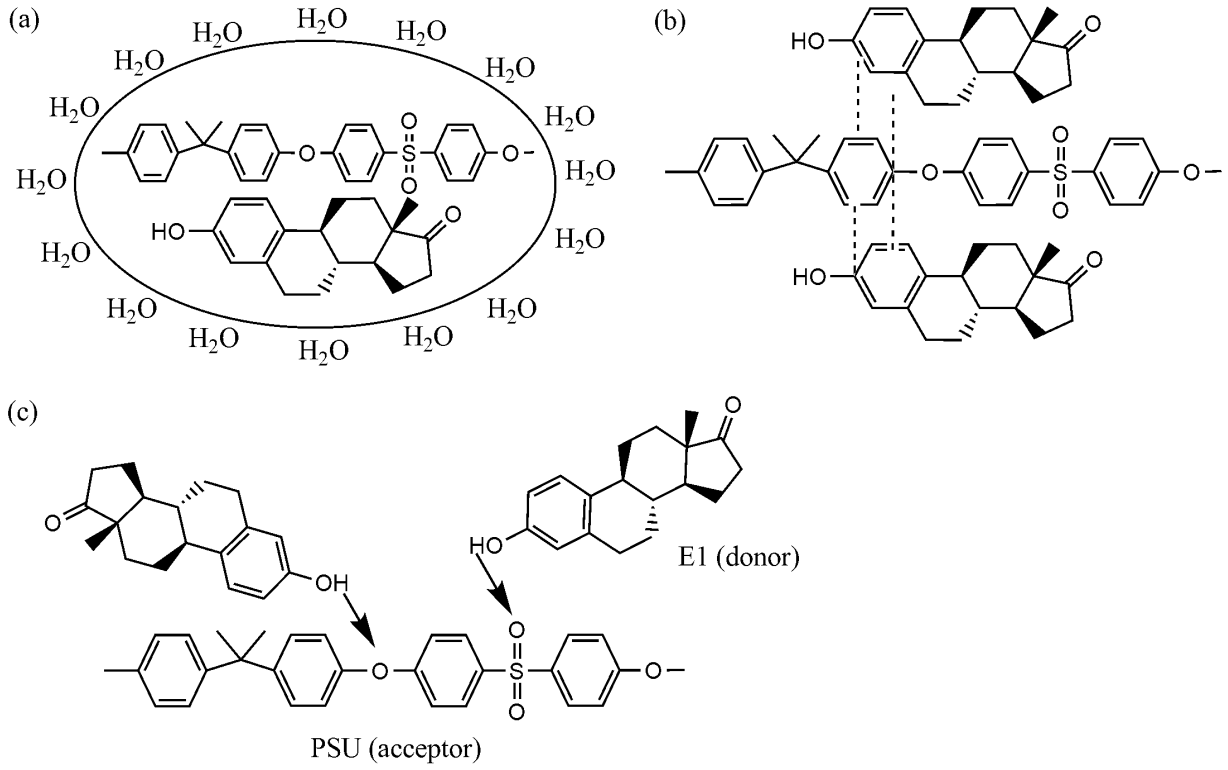

Figure 6. Schematic representation of the possible different interaction mechanisms between PSU nanofibers and E1 hormone; (a) hydrophobic interactions, (b) π–π stacking interaction, and (c) hydrogen bonding. Strong bonding interactions are represented with bold arrows, while weak interactions are represented with dotted lines.

Therefore, comparing the types of adsorption interaction mechanisms between estrogenic hormones and PSU nanofibers with PLA and PVDF, the overall descending trend of hormones adsorption on nanofibers is as PSU >PLA >PVDF, which is also evident from Figure 3a.

3.6. Thermodynamic study

The thermodynamic parameters were estimated by plotting a Van't Hoff plot of lnK_D versus $1/T$, while values of ΔS and ΔH were determined from the slope and intercept, respectively. Values of ΔG at different temperatures were then calculated and are given in Table 4.

Table 4

Thermodynamic parametric values for the adsorption of E1 hormone.

Parameters	**Temperature**

	298 K	*308 K*	*318 K*
ΔG° (kJ/mol)	-0.596	-0.566	-0.536
ΔH° (kJ/mol)		-1.478	
ΔS° (J/mol K)		-2.958	

In general, the adsorption capacities of the PSU sample decreased at higher temperatures (Figure 5d). The highest increase in adsorption capacity occurred by increasing the temperature from 25 to 35 °C. This increase in temperature may have facilitated diffusion of the hormone molecules through the spun PSU material's matrix, thereby favoring adsorption. The calculated thermodynamic parameters from Eq. (8), (9), and (10) summarized in Table 4 depicted ΔH and ΔG values to be negative. This indicated that the adsorption process of the estrogenic hormone onto PSU was exothermic and spontaneous, demonstrating favourability at lower temperatures. The values of ΔG ranging from −0.536 to −0.59 kJ/mol, imply that evaluated estrogenic hormones were adsorbed onto PSU through the mechanism of physical adsorption. The ΔH value (≤ 20 kJ/mol) determined for the hormone adsorption on PSU also suggested that adsorption occurred through the mechanism of physical adsorption [58]. The negative ΔS entropy value suggested a decrease in randomness at the solute/solid interface.

3.7. Isotherm modeling

By plotting q_e vs. C_e, the equilibrium adsorption data were fitted with isotherm models as presented in Figure 7, while the calculated isothermic parameters are given in Table 5.

The Langmuir model is based on the assumption of monolayer coverage on a homogenous surface with identical adsorption sites, given there is no interaction between the adsorbate molecules, while the Freundlich model describes multilayer adsorption with the interaction between adsorbate molecules and heterogeneous adsorbent surface for various adsorption sites [63,64]. Adsorption capacities of spun PSU increased with initial hormone concentration, although the characteristic plateau was not achieved in the investigated concentration range. According to R^2 values (> 0.990), both models fit well with the experimental. This was supported by the low values obtained for the other error analysis parameters (Sum of squared errors and Chi-squared). However, the experimental data best fitted with the Freundlich isotherm model. This indicates that the adsorption

of the hormones on the surface of PSU was mainly heterogeneous. Freundlich parameter K_F is an indication of the PSU capacity, while *n* is a measure of the surface heterogeneity. For the investigated hormone, the *n* value was below one, indicating the heterogeneous surface of the adsorbent. Maximum adsorption capacities calculated from the Langmuir isotherm was 10.65 mg/g for hormone, which was in close agreement with that calculated from the combined Langmuir-Freundlich isotherms was 12.88 mg/g, indicating the suitability of these isotherms in describing the adsorption process of the hormone on the adsorbent. Similar results for the same hormone have been reported by Patel *et al.* [60] and Prokic *et al.* [47], with maximum adsorption capacities determined as 10.12 mg/g and 12.66 mg/g, respectively.

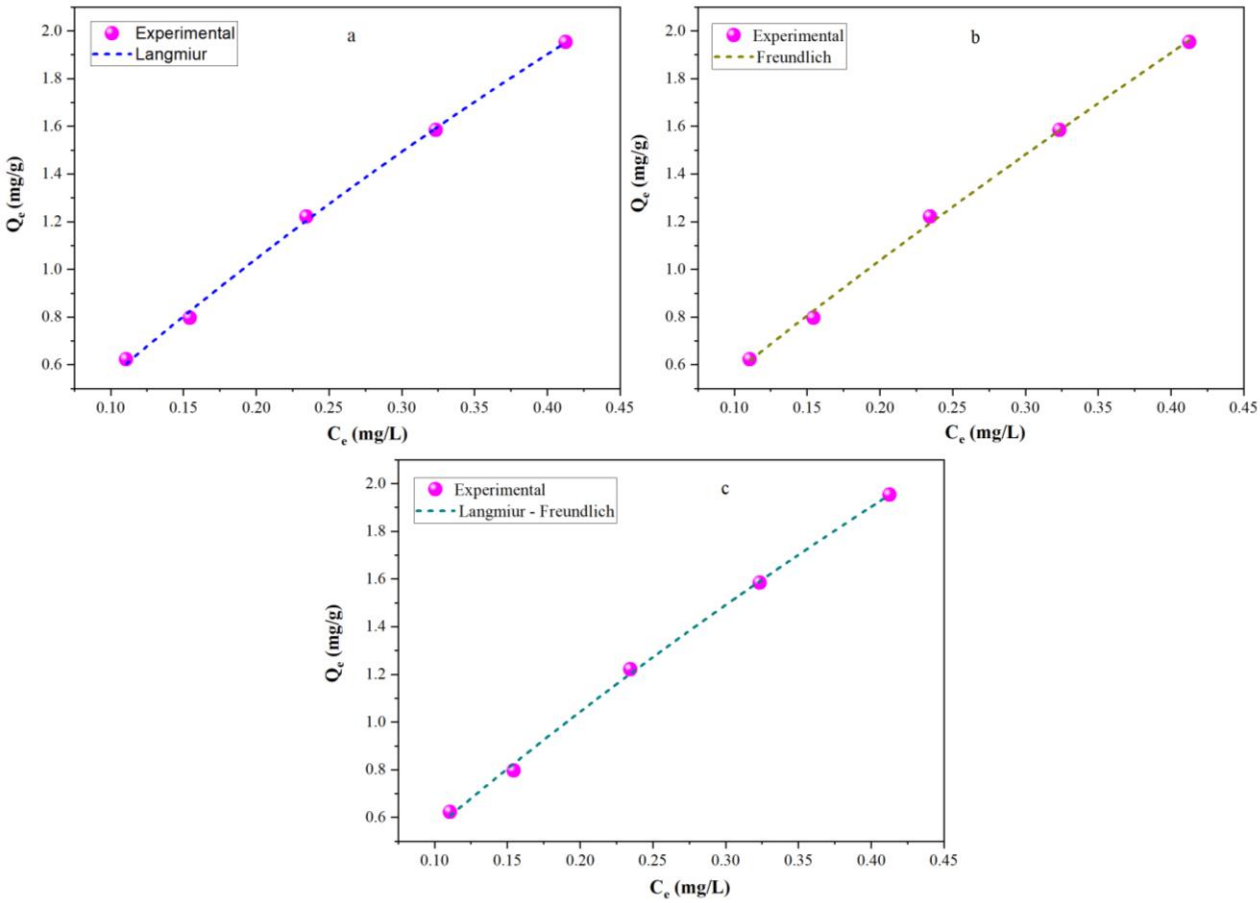

Figure 7. Adsorption isotherms for E1 hormone using PSU electrospun nanofibers; a) Langmuir, b) Freundlich and c) Langmuir-Freundlich model.

Table 5

Calculated adsorption isotherm parameters for the adsorption of the E1 hormone.

Langmuir model					
Q_{max} (mg/g)	K_L (L/mg)	R_L	R^2	SSE	χ^2
10.651	0.543	0.696 – 0.887	0.998	0.00144	0.00048
Freundlich model					
K_F (mg/g)(L/mg)		n	R^2	SSE	χ^2
4.267		0.878	0.999	0.00172	0.00057
Langmuir – Freundlich model					
Q_{max} (mg/g)	K_{LF}	n	R^2	SSE	χ^2
12.888	0.424	0.975	0.996	0.00142	0.00071

SSE = Sum of squared errors, χ^2 = Chi-square

3.8. A comparative study with other adsorbents

The following Table 6 compares the reported electrospun nanofibers and other adsorbents particles reported in the literature for effective removal of E1 hormone.

Table 6

Comparison of adsorption capacity of E1 hormone using PSU to various adsorbents.

Material	**Hormone**	**pH and Temperature (°C)**	**Adsorption capacity (mg/g)**	**Reference**
PES nanofibers	E1	7 and 25	0.442	39
PAN nanofibers	E1	7 and 25	0.396	39
PA nanofibers	E1	7 and 25	0.331	39
MWCNTs	E1	7 and 25	0.423	43
Activated sludge	E1	7 and 25	0.002533	43
Hydrophobic hollow fiber membrane	E1	7 and 25	0.000062	43
Carbonized hydrothermal carbon	E1	7 and 25	0.95	48
PSU nanofibers	E1	7 and 25	0.508	**Present study**

PSU possesses a high adsorption capacity owing to its surface area of 6.3 m^2/g, which is relatively low for the other compared materials reported in the literature. The results revealed that PSU nanofibers at pH 7 and room temperature (25 °C) possessed a cumulative adsorption capacity of 2.115 mg/g with an individual adsorption capacity of E1 to be 0.508 mg/g. This value is higher than the adsorption capacity of the compared electrospun nanofibers, MWCNTs, activated sludge,

and hollow fiber membrane shown in Table 6. However, the value is slightly low compared to carbonized hydrothermal carbon owing to its high surface area compared to electrospun nanofibers based on the nature of that material. When comparing PSU with the other electrospun nanofiber reported in the literature, the value for PSU nanofibers is high owing to its high surface area and small average fiber diameter of 183 ± 32 nm (PES: 199 ± 51 nm, PAN: 330 ± 73, PA: 220 ± 51 nm), the structure that allows hydrophobic and π–π interactions, and functional groups present on the surface that facilitate hydrogen bonding with E1 hormone, as discussed in adsorption mechanism.

3.9. Adsorption-desorption study

It can be seen in Figure 8 that the highest adsorption was achieved at around 82.2%, which was gradually reduced, reaching the efficiency of about 60% in six adsorption cycles which is evidence of the high performance of PSU nanofibers. Similarly, desorption cycles followed the same trend; however, the efficiency remained slightly higher in most of the cycles using desorption of E1 from PSU nanofibers which clearly indicates the effectiveness of the process for recovery of E1 hormones from the nanofibers. Additionally, The SEM image shows surface morphology of nanofibers after six cycles. A slight increase in the diameter of nanofiber is observed rising from 183 to 246 nm. A plausible reason of swelling is attributed to the interaction of nanofiber with the ethanol while in contact during the desorption cycles [39].

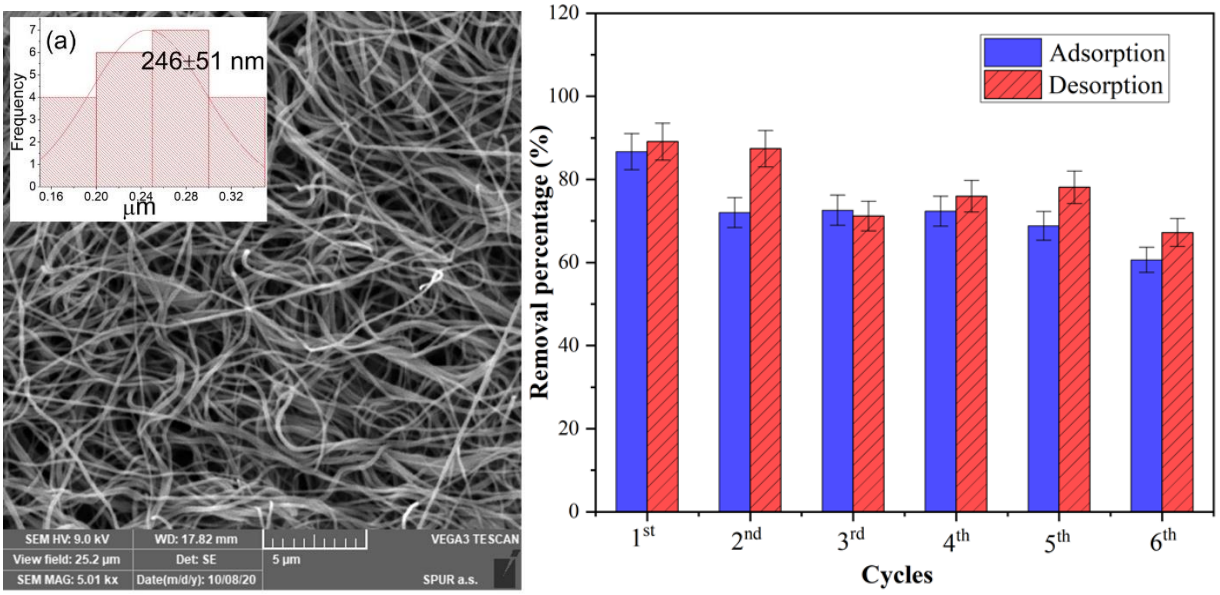

Figure 8. SEM micrograph after study with (inset) distribution of the fiber diameter (in the left panel) and cycles of adsorption-desorption for E1 by PSU nanofibers (in the right panel).

4. Conclusions

Polymeric nanofibers that include PSU, PLA, and PVDF were successfully produced via the facile electrospinning method and could adsorb all types of estrogenic hormones. These fibers possessed a mean fiber diameter of 149 - 183 nm and a specific surface area of 1.6 - 6.3 m^2/g. The preliminary study showed that PSU was the best among these polymers, with the highest percentage of removal (71.2%) of E1. The adsorption of hormones on PSU is significantly high compared to other polymers owing to the hydrogen bonding interactions. Therefore, five models (pseudo-first-order, pseudo-second-order, intraparticle diffusion, Elovich, and fractional power model) were deployed on experimental data to obtain the adsorption kinetics and to understand the characteristics of PSU fibers with contact time. The obtained results showed that E3 followed pseudo-first-order kinetics while E1, E2, and EE2 best fitted pseudo-second-order kinetics. It was found that PSU fibers had maximum removal efficiency of 71.2, 65.9, 56.9, and 36.1 % for E1, EE2, E2, and E3, respectively. Adsorption obeyed Langmuir-Freundlich isothermal adsorption models; thermodynamics and mechanisms were evaluated, revealing that the adsorption process of E1 was exothermic and spontaneous in nature. The adsorption-desorption cycles were conducted over six cycles to determine the reusability and effectiveness of PSU, which remained above 60%. Overall, the results indicate that PSU can be a potential and efficient adsorbent for the effective simultaneous removal of estrogenic hormones from water streams.

Acknowledgements

The authors gratefully acknowledge the financial support from the Ministry of Education, Youth, and Sports of the Czech Republic (RP/CPS/2022/002 and RP/CPS/2022/005), the Internal Grant Agency of TBU in Zlin (grant no. IGA/CPS/2022/003). We would also like to acknowledge the Centre of Polymer Systems (CPS) situated at Tomas Bata University in Zlin, Czech Republic, to use the available research facilities to conduct this research work.

Conflict of interest

The authors declare there exist no form of competing interests.

CrediT authorship contribution statement

Muhammad Yasir: Conceptualization, Methodology, Investigation, Formal analysis, Data curation, Writing- original draft, Writing- Review & editing.

Fahanwi Asabuwa Ngwabebhoh: Formal analysis, Data curation, Writing- Review & editing.

Tomáš Šopík: Methodology, Formal analysis, Data curation.

Lenka Lovecka: Formal analysis, Data curation.

Dušan Kimmer: Conceptualization, Supervision, Review & editing.

Vladimír Sedlařík: Conceptualization, Supervision, Project administration, Funding acquisition, Review & editing.

References

1. AlAbduljabbar FA, Haider S, Ali FAA, Alghyamah AA, Almasry WA, Patel R, et al. Efficient Photocatalytic Degradation of Organic Pollutant in Wastewater by Electrospun Functionally Modified Polyacrylonitrile Nanofibers Membrane Anchoring TiO2 Nanostructured. Membranes (Basel). 2021 Oct;11(10):785.

2. Wu X, Cobbina SJ, Mao G, Xu H, Zhang Z, Yang L. A review of toxicity and mechanisms of individual and mixtures of heavy metals in the environment. Environ Sci Pollut Res. 2016 May;23(9):8244–59.

3. Hamid N, Junaid M, Pei D-S. Combined toxicity of endocrine-disrupting chemicals: A review. Ecotoxicol Environ Saf. 2021 Jun;215:112136.

4. Haddaoui I, Mateo-Sagasta J. A review on occurrence of emerging pollutants in waters of the MENA region. Environ Sci Pollut Res. 2021 Dec;28(48):68090–110.

5. Balali-Mood M, Naseri K, Tahergorabi Z, Khazdair MR, Sadeghi M. Toxic Mechanisms of Five Heavy Metals: Mercury, Lead, Chromium, Cadmium, and Arsenic . Vol. 12, Frontiers in Pharmacology . 2021.

6. Kocour Kroupová H, Valentová O, Svobodová Z, Šauer P, Máchová J. Toxic effects of nitrite on freshwater organisms: a review. Rev Aquac. 2018 Aug;10(3):525–42.

7. Chambers WS, Hopkins JG, Richards SM. A Review of Per- and Polyfluorinated Alkyl Substance Impairment of Reproduction . Vol. 3, Frontiers in Toxicology . 2021.

8. La Merrill MA, Vandenberg LN, Smith MT, Goodson W, Browne P, Patisaul HB, et al. Consensus on the key characteristics of endocrine-disrupting chemicals as a basis for hazard identification. Nat Rev Endocrinol. 2020 Jan;16(1):45–57.

9. Hilakivi-Clarke L, de Assis S, Warri A. Exposures to synthetic estrogens at different times during the life, and their effect on breast cancer risk. J Mammary Gland Biol Neoplasia. 2013/02/08. 2013 Mar;18(1):25–42.

10. Czarny K, Szczukocki D, Krawczyk B, Gadzała-Kopciuch R, Skrzypek S. Toxicity of single steroid hormones and their mixtures toward the cyanobacterium Microcystis aeruginosa. J Appl Phycol. 2019;31(6):3537–44.

11. Street ME, Angelini S, Bernasconi S, Burgio E, Cassio A, Catellani C, et al. Current knowledge on endocrine disrupting chemicals (EDCs) from animal biology to humans, from pregnancy to adulthood: Highlights from a national italian meeting. International Journal of Molecular Sciences. 2018.

12. Kumar M, Sarma DK, Shubham S, Kumawat M, Verma V, Prakash A, et al. Environmental Endocrine-Disrupting Chemical Exposure: Role in Non-Communicable Diseases . Vol. 8, Frontiers in Public Health . 2020.

13. Henley D V, Lindzey J, Korach KS. Steroid Hormones. In: Melmed S, Conn PM, editors. Endocrinology. Totowa, NJ: Humana Press; 2005. p. 49–65.

14. Koh YKK, Chiu TY, Boobis A, Cartmell E, Scrimshaw MD, Lester JN. TREATMENT AND REMOVAL STRATEGIES FOR ESTROGENS FROM WASTEWATER. Environ Technol. 2008 Mar;29(3):245–67.

15. Gao X, Kang S, Xiong R, Chen M. Environment-Friendly Removal Methods for Endocrine Disrupting Chemicals. Sustainability. 2020 Sep;12(18):7615.

16. Muhammad Y, Milan M, Tomas S, Hassan A, Michal U, Jan A, et al. ZnO nanowires and

nanorods based ZnO/WO3/Pt heterojunction for efficient photocatalytic degradation of Estriol (E3) hormone. Mater Lett [Internet]. 2022;319(April):132291. Available from: https://doi.org/10.1016/j.matlet.2022.132291

17. Yasir M, Sopik T, Patwa R, Kimmer D, Sedlarik V. Adsorption of estrogenic hormones in aqueous solution using electrospun nanofibers from waste cigarette butts : Kinetics, mechanism, and reusability. Express Polym Lett. 2022;16(6):624–48.

18. Hartmann J, Beyer R, Harm S. Effective Removal of Estrogens from Drinking Water and Wastewater by Adsorption Technology. Environ Process. 2014;1(1):87–94.

19. Peiris C, Nawalage S, Wewalwela JJ, Gunatilake SR, Vithanage M. Biochar based sorptive remediation of steroidal estrogen contaminated aqueous systems: A critical review. Environ Res. 2020;191:110183.

20. Ogata F, Tominaga H, Yabutani H, Kawasaki N. Removal of Estrogens from Water Using Activated Carbon and Ozone. J Oleo Sci. 2011;60(12):609–11.

21. Wang X, Liu N, Liu Y, Jiang L, Zeng G, Tan X, et al. Adsorption Removal of 17β-Estradiol from Water by Rice Straw-Derived Biochar with Special Attention to Pyrolysis Temperature and Background Chemistry. Vol. 14, International Journal of Environmental Research and Public Health . 2017.

22. O. Ifelebuegu A. Removal of Steriod Hormones by Activated Carbon Adsorption—Kinetic and Thermodynamic Studies. J Environ Prot (Irvine, Calif). 2012;

23. Jiang L, Liu Y, Liu S, Zeng G, Hu X, Hu X, et al. Adsorption of Estrogen Contaminants by Graphene Nanomaterials under Natural Organic Matter Preloading: Comparison to Carbon Nanotube, Biochar, and Activated Carbon. Environ Sci Technol. 2017 Jun;51(11):6352–9.

24. Cheng C, Li X, Yu X, Wang M, Wang X. Chapter 14 - Electrospun Nanofibers for Water Treatment. In: Ding B, Wang X, Yu JBT-EN and A, editors. Micro and Nano Technologies. William Andrew Publishing; 2019. p. 419–53.

25. Agrawal S, Ranjan R, Lal B, Rahman A, Singh SP, Selvaratnam T, et al. Synthesis and

Water Treatment Applications of Nanofibers by Electrospinning. Vol. 9, Processes . 2021.

26. Matei E, Covaliu-Mierla CI, Ţurcanu AA, Râpă M, Predescu AM, Predescu C. Multifunctional Membranes—A Versatile Approach for Emerging Pollutants Removal. Vol. 12, Membranes . 2022.

27. Mat Nawi NI, Chean HM, Shamsuddin N, Bilad MR, Narkkun T, Faungnawakij K, et al. Development of Hydrophilic PVDF Membrane Using Vapour Induced Phase Separation Method for Produced Water Treatment. Vol. 10, Membranes . 2020.

28. Goetz LA, Naseri N, Nair SS, Karim Z, Mathew AP. All cellulose electrospun water purification membranes nanotextured using cellulose nanocrystals. Cellulose. 2018;25(5):3011–23.

29. Liu L, Lin Z, Niu J, Tian D, He J. Electrospun polysulfone/poly(lactic acid) nanoporous fibrous mats for oil removal from water. Adsorpt Sci Technol. 2019 Feb;37(5–6):438–50.

30. Rosalam S, Chiam CK, Widyaparamitha S, Chang YW, Lee CA. Water desalination by air-gap membrane distillation using meltblown polypropylene nanofiber membrane. IOP Conf Ser Earth Environ Sci. 2016;36:12032.

31. Li X, García-Payo MC, Khayet M, Wang M, Wang X. Superhydrophobic polysulfone/polydimethylsiloxane electrospun nanofibrous membranes for water desalination by direct contact membrane distillation. J Memb Sci. 2017 Nov;542:308–19.

32. Rahman ROA, El-Kamash AM, Hung Y-T. Applications of Nano-Zeolite in Wastewater Treatment: An Overview. Vol. 14, Water . 2022.

33. Ivanoska-Dacikj A, Makreski P, Bogoeva-Gaceva G. Fabrication of biodegradable polyurethane electrospun webs of fibers modified with biocompatible graphene oxide nanofiller. J Ind Text. 2021 Mar;152808372110031.

34. Almasian A, Chizari Fard G, Parvinzadeh Gashti M, Mirjalili M, Mokhtari Shourijeh Z. Surface modification of electrospun PAN nanofibers by amine compounds for adsorption of anionic dyes. Desalin Water Treat. 2016 May;57(22):10333–48.

35. Han J, Qiu W, Gao W. Adsorption of estrone in microfiltration membrane filters. Chem Eng J [Internet]. 2010;165(3):819–26. Available from: http://dx.doi.org/10.1016/j.cej.2010.10.024

36. Han J, Qiu W, Cao Z, Hu J, Gao W. Adsorption of ethinylestradiol (EE2) on polyamide 612: Molecular modeling and effects of water chemistry. Water Res [Internet]. 2013;47(7):2273–84. Available from: http://www.sciencedirect.com/science/article/pii/S0043135413000766

37. Schäfer AI, Stelzl K, Faghih M, Sen Gupta S, Krishnadas KR, Heißler S, et al. Poly(ether sulfone) Nanofibers Impregnated with β-Cyclodextrin for Increased Micropollutant Removal from Water. ACS Sustain Chem Eng. 2018;6(3):2942–53.

38. Wang M, Qu F, Jia R, Sun S, Li G, Liang H. Preliminary study on the removal of steroidal estrogens using TiO2-doped PVDF ultrafiltration membranes. Water (Switzerland). 2016;8(4):1–12.

39. Yasir M, Šopík T, Lovecká L, Kimmer D, Sedlařík V. The adsorption, kinetics, and interaction mechanisms of various types of estrogen on electrospun polymeric nanofiber membranes. Nanotechnology [Internet]. 2021;33(7):75702. Available from: http://dx.doi.org/10.1088/1361-6528/ac357b

40. Qi FF, Cao Y, Wang M, Rong F, Xu Q. Nylon 6 electrospun nanofibers mat as effective sorbent for the removal of estrogens: Kinetic and thermodynamic studies. Nanoscale Res Lett. 2014;9(1):1–10.

41. Ersali S, Hadadi V, Moradi O, Fakhri A. Pseudo-second-order kinetic equations for modeling adsorption systems for removal of ammonium ions using multi-walled carbon nanotube. Fullerenes, Nanotub Carbon Nanostructures. 2013;150527104639002.

42. Tian Y, Wu M, Liu R, Li Y, Wang D, Tan J, et al. Electrospun membrane of cellulose acetate for heavy metal ion adsorption in water treatment. Carbohydr Polym [Internet]. 2011;83(2):743–8. Available from: http://dx.doi.org/10.1016/j.carbpol.2010.08.054

43. Al-Khateeb LA, Obaid AY, Asiri NA, Abdel Salam M. Adsorption behavior of estrogenic

compounds on carbon nanotubes from aqueous solutions: Kinetic and thermodynamic studies. J Ind Eng Chem [Internet]. 2014;20(3):916–24. Available from: http://dx.doi.org/10.1016/j.jiec.2013.06.023

44. Ho YS, McKay G. Application of kinetic models to the sorption of copper (II) on to peat. Adsorpt Sci Technol. 2002;20(8):797–815.

45. Ngwabebhoh FA, Mammadli N, Yildiz U. Bioinspired modified nanocellulose adsorbent for enhanced boron recovery from aqueous media: Optimization, kinetics, thermodynamics and reusability study. J Environ Chem Eng [Internet]. 2019;7(5):103281. Available from: https://doi.org/10.1016/j.jece.2019.103281

46. Carballa M, Fink G, Omil F, Lema JM, Ternes T. Determination of the solid-water distribution coefficient (Kd) for pharmaceuticals, estrogens and musk fragrances in digested sludge. Water Res. 2008;42(1–2):287–95.

47. Prokić D, Vukčević M, Kalijadis A, Maletić M, Babić B, Đurkić T. Removal of Estrone, 17β-Estradiol, and 17α-Ethinylestradiol from Water by Adsorption onto Chemically Modified Activated Carbon Cloths. Fibers Polym. 2020;21(10):2263–74.

48. Proki D, Vuk M, Mitrovi A, Maleti M, Kalijadis A, Jankovi I, et al. from water onto modified multi-walled carbon nanotubes , carbon cryogel , and carbonized hydrothermal carbon. 2021;

49. Ngwabebhoh FA, Erdem A, Yildiz U. Synergistic removal of Cu(II) and nitrazine yellow dye using an eco-friendly chitosan-montmorillonite hydrogel: Optimization by response surface methodology. J Appl Polym Sci. 2016;133(29):1–14.

50. M. Yasir, F. A. Ngwabebhoh, T. Sopik, H. Ali, V. Sedlarik. Electrospun polyurethane nanofibers coated with polyaniline / polyvinyl alcohol as ultrafiltration membranes for the removal of ethinylestradiol hormone micropollutant from aqueous phase. J Environ Chem Eng. 2022;10(3):107811.

51. Kaspar P, Sobola D, Částková K, Knápek A, Burda D, Orudzhev F, et al. Characterization of polyvinylidene fluoride (Pvdf) electrospun fibers doped by carbon flakes. Polymers

(Basel). 2020;12(12):1–15.

52. Lanceros-Méndez S, Mano JF, Costa AM, Schmidt VH. FTIR and DSC studies of mechanically deformed β-PVDF films. J Macromol Sci - Phys. 2001;40 B(3–4):517–27.

53. Sengupta D, Kottapalli AGP, Chen SH, Miao JM, Kwok CY, Triantafyllou MS, et al. Characterization of single polyvinylidene fluoride (PVDF) nanofiber for flow sensing applications. AIP Adv. 2017;7(10).

54. Sepahi S, Kalaee M, Mazinani S, Abdouss M, Hosseini SM. Introducing electrospun polylactic acid incorporating etched halloysite nanotubes as a new nanofibrous web for controlled release of Amoxicillin. J Nanostructure Chem [Internet]. 2021;11(2):245–58. Available from: https://doi.org/10.1007/s40097-020-00362-w

55. Rosid SM, Ajji A, Hasbullah H, Rosid SJM, Ismail AF, Goh PS. Physicochemical characteristics of polysulfone nanofiber membranes with iron oxide nanoparticles via electrospinning. J Appl Polym Sci. 2022;139(8):1–10.

56. Mazoochi T, Hamadanian M, Ahmadi M, Jabbari V. Investigation on the morphological characteristics of nanofiberous membrane as electrospun in the different processing parameters. Int J Ind Chem. 2012;3(1):1–8.

57. Schäfer AI, Akanyeti I, Semião AJC. Micropollutant sorption to membrane polymers: A review of mechanisms for estrogens. Adv Colloid Interface Sci [Internet]. 2011;164(1–2):100–17. Available from: http://dx.doi.org/10.1016/j.cis.2010.09.006

58. Duan Q, Li X, Wu Z, Alsaedi A, Hayat T, Chen C, et al. Adsorption of 17β-estradiol from aqueous solutions by a novel hierarchically nitrogen-doped porous carbon. J Colloid Interface Sci [Internet]. 2019;533:700–8. Available from: https://doi.org/10.1016/j.jcis.2018.09.007

59. Zhang J, Nguyen MN, Li Y, Yang C, Schäfer AI. Steroid hormone micropollutant removal from water with activated carbon fiber-ultrafiltration composite membranes. J Hazard Mater [Internet]. 2020;391(September 2019):122020. Available from: https://doi.org/10.1016/j.jhazmat.2020.122020

60. Patel S, Han J, Gao W. Sorption of 17β-estradiol from aqueous solutions on to bone char derived from waste cattle bones: Kinetics and isotherms. J Environ Chem Eng [Internet]. 2015;3(3):1562–9. Available from: http://dx.doi.org/10.1016/j.jece.2015.04.027

61. Gong K, Lin Y, Wu P, Jin X, Owens G, Chen Z. Removal mechanism of 17β-estradiol by carbonized green synthesis of Fe/Ni nanoparticles. Chemosphere [Internet]. 2022;291(P2):132777. Available from: https://doi.org/10.1016/j.chemosphere.2021.132777

62. Jin X, Hu J. Role of water chemistry on estrone removal by nanofiltration with the presence of hydrophobic acids. Front Environ Sci Eng. 2015;9(1):164–70.

63. Tagliavini M, Engel F, Weidler PG, Scherer T, Schäfer AI. Adsorption of steroid micropollutants on polymer-based spherical activated carbon (PBSAC). J Hazard Mater [Internet]. 2017;337:126–37. Available from: http://dx.doi.org/10.1016/j.jhazmat.2017.03.036

64. Ngwabebhoh FA, Gazi M, Oladipo AA. Adsorptive removal of multi-azo dye from aqueous phase using a semi-IPN superabsorbent chitosan-starch hydrogel. Chem Eng Res Des [Internet]. 2016;112:274–88. Available from: http://dx.doi.org/10.1016/j.cherd.2016.06.023